Electrophoretic Deposition of One- and Two-Layers Compacts of Holmium and Yttrium Oxide Nanopowders for Magneto-optical Ceramics Fabrication

Elena G. Kalinina , Nataliya D. Kundikova , Dmitrii K. Kuznetsov , Maxim G. Ivanov *

Posted Date: 30 August 2023

doi: 10.20944/preprints202308.2043.v1

Keywords: magnetooptical ceramics; electrophoretic deposition (EPD); two-layer ceramics; holmium oxide; yttrium oxide

Article

Electrophoretic Deposition of One- and Two-Layers Compacts of Holmium and Yttrium Oxide Nanopowders for Magneto-Optical Ceramics Fabrication

E.G. Kalinina [1,2,3], N.D. Kundikova [1,4], D.K. Kuznetsov [2] and M.G. Ivanov [1,3,*]

[1] Institute of Electrophysics, Ural Branch of Russian Academy of Sciences, 106 Amundsen str., Ekaterinburg, 620016, Russia;
[2] Ural Federal University, 19 Mira Avenue, Ekaterinburg, 620002, Russia;
[3] G.G. Devyatykh Institute of Chemistry of High-Purity Substances, Russian Academy of Sciences, 49 Tropinin Str., Nizhny Novgorod, Russia;
[4] South Ural State University, 76 Lenin prospekt, Chelyabinsk, 454080, Russia
* Correspondence: author E-mail address: max@iep.uran.ru (Maxim Ivanov)

Abstract: In this work, the possibility of fabrication composite magneto-optical ceramics by electrophoretic deposition (EPD) of nanopowders and high temperature vacuum sintering of the compacts was investigated. Holmium oxide was chosen as a magneto-optical material for the study because of its transparency in the mid-IR range. Nanopowders of magnetooptical $(Ho_{0.95}La_{0.05})_2O_3$ (HoLa) material were made by self-propagating high-temperature synthesis. Nanopowders of $(Y_{0.9}La_{0.1})_2O_3$ (YLa) for an inactive matrix were made by laser synthesis. A process of formation of one- and two-layers compacts by the EPD of the nanopowders from alcohol suspensions was studied in details. Acetylacetone was shown to be a good dispersant to obtain alcohol suspensions of the nanopowders characterized by high zeta potential values (+29 – +80 mV) and carry out a stable EPD process. One-layer compacts were made from the HoLa and YLa nanopowders with a density of 30–43%. It was found out that the introduction of polyvinyl butyral (PVB) into the suspension leads to a decrease in the mass and thickness of the green bodies deposited, but does not significantly affect their density. A possibility to make two-layers (YLa/HoLa) compacts with a thickness of up to 2.6 mm and a density of up to 46% was demonstrated. Sintering such compacts in a vacuum at a temperature of 1750°C for 10 hours leads to the formation of ceramics with a homogeneous boundary between the YLa/HoLa layers and thickness of the interdiffused ions layer of about 30 μm.

Keywords: magnetooptical ceramics; electrophoretic deposition (EPD); two-layer ceramics; holmium oxide; yttrium oxide

1. Introduction

One of challenges of magneto-optical devices fabrication is to increase the maximum allowable power of laser radiation in Faraday isolators [1]. When a laser beam passes through a magneto-optical element, heat is inevitably released, thermally induced polarization and phase distortions appear, which leads to a deterioration in the quality of the laser beam and a decrease in the insulating ability of the device. This problem can be solved by new designs of magneto-optical elements, in particular, by creating a composite structure. Traditionally, magneto-optical elements have a rod configuration with radial cooling. In this case, the higher the power of the transmitted radiation and the lower the thermal conductivity of the material, the greater the temperature difference between the central and peripheral parts of the optical element, and the greater the thermally induced distortions (thermal

lens, etc.). In laser technology, the problem of reducing the thermal lens can be solved by organizing efficient heat removal by creating a composite element consisting of an active medium and an inactive matrix, for example: YAG/Nd:YAG/YAG [2], YAG/Yb:YAG/YAG [3], Yb:YAG/YAG [4,5], Er:YAG/YAG [6] or a material with a noticeably higher thermal conductivity, for example: Yb:YAG/sapphire [4], Nd:YAG/diamond [7]. In these cases, the released heat is effectively removed from the active medium, reducing the radial temperature gradient, which makes it possible to increase the laser radiation power and/or provide less distortion of the laser beam. With the development of optical ceramic technologies, this approach is being used in active laser elements, but we are not aware of the implementation of such an approach for magneto-optical elements.

One of the promising magneto-optical materials to use in the mid-IR range is holmium oxide [1], the possibility of obtaining transparent ceramics of which was recently shown in [8]. Usually, to obtain optically transparent ceramics from sesquioxides, such methods as slip casting [9] and isostatic pressing followed by vacuum sintering [8], hot pressing (HP) [10–12], hot isostatic pressing (HIP) [13–17], spark plasma sintering (SPS) [18,19] are used. Hot pressing methods require expensive technological equipment, and also have a number of disadvantages associated with contamination of the ceramics, appearance of mechanical defects and internal stresses. Among relatively cheap forming methods that give a chance to obtain large size dense unstressed compacts (green bodies) needed for further sintering of the transparent ceramics, one can single out a method of slip [20] or tape [6] casting, based on preparation of concentrated suspensions of nanoparticles with the help of dispersants and polymer binders. However, it should be noted that the burnout of the polymers at the sintering stage can lead to the formation of light-scattering defects inside the ceramics.

Relatively recently, it was shown that a promising method for the formation of transparent ceramics is the method of electrophoretic deposition (EPD) [21], which has a high deposition rate, the possibility of using powders of various compositions and size distribution, gives a chance for thickness control (from thin films to bulk compacts) and sample morphology by changing the deposition parameters (applied voltage and current, deposition time). Preparation of stable powder suspensions is an important step in the implementation of the EPD process. The degree of stability of suspensions is characterized by the electrokinetic zeta potential and the value of the zeta potential can be controlled by using dispersants, for example, acetylacetone, polyethyleneimine, ammonium polyacrylate, etc. [22]. Talking about stabilization of the nanoparticles in the suspensions, it should be noted that when using the EPD to obtain dense ceramic green body, one has to solve a contradictory task. On the one hand, suspensions must be stable during the entire EPD process, i.e. the particles should repel each other and not flocculate, and on the other hand, after deposition on the electrode, the particles should form an “ideal” dense packed structure. In the works [23,24] a possibility of sintering optical ceramics based on $(La_xY_{1-x})_2O_3$ solid solutions, where lanthanum oxide was used as a sintering aid, from green bodies with a relatively low density (30 – 40%) made by the EPD from isopropyl alcohol suspensions of nanoparticles produced by laser synthesis was shown.

In this work, we systematically studied the processes of the formation of bulk single-layer and two-layer compacts by the EPD method from non-aqueous suspensions using a dispersant (acetylacetone) and a polymeric binder (polyvinyl butyral) based on $(Y_{0.9}La_{0.1})_2O_3$ (YLa) nanopowders obtained by laser synthesis and $(Ho_{0.95}La_{0.05})_2O_3$ (HoLa) obtained by self-propagating high-temperature synthesis (SHS). The main objectives of the research were to determine the effect of the dispersant and the binder on the zeta potential, the current during the EPD, the mass and density of the green bodies, and also to study the possibility of sintering the two-layer ceramics.

2. Materials and Methods

2.1. Nanopowders and Suspensions of $(Y_{0.9}La_{0.1})_2O_3$

Two batches of nanopowders of $(Y_{0.9}La_{0.1})_2O_3$ (*YLa*) solid solutions were obtained by evaporating the material with ytterbium fiber laser radiation at a wavelength of 1.07 μm. The process is described in detail in [23,25]. The material to evaporate was mixed from commercially available powders of high purity yttrium and lanthanum oxides (99.99% Polirit, Russia), pressed into cylindrical targets,

60 mm in diameter and 20 mm thick, and sintered in air at a temperature of 1300°C for 1 h. The targets were evaporated under the pulsed laser radiation with a pulse repetition rate of 2 kHz, the pulse duration of 60 μs, and an average power of 250 W. The evaporation chamber was blown through with air of atmospheric pressure at a flow rate of 40 L/min. The nanopowders carried away by the air stream were collected in a cyclone and an electrostatic filter. The specific surface area of the *YLa* nanopowders collected in a cyclone and an electrostatic precipitator was 76 m^2/g and 80 m^2/g, respectively, and the batches of the nanopowders were accordingly named *76YLa* and *80YLa*. The specific surface area of the *YLa* nanopowders collected in a cyclone and an electrostatic precipitator was determined by the BET method (TriStar 3000, Micromeritics, USA). All obtained powders were annealed in air at 900°C for 3 h in a camber furnace (LHT 02/18, Nabertherm, Germany). The XRD was recorded with a D8 DISCOVER GADDS (Bruker AXS, Germany) with Cu ($K_{\alpha 1,2}$ λ = 1,542Å) radiation and a carbon monochromator. The XRD data were analyzed using the TOPAS 3 software (Bruker AXS, Germany) with Rietveld's algorithm to specify structure parameters.

To prepare the suspensions, isopropanol (special purity grade, JSC "Component-Reaktiv", Moscow, Russia) (iPrOH) was used as a dispersion medium. Suspensions of 80YLa with an initial concentration of 70 g/L were prepared using an ultrasonic bath (UZV-13/150-TN, Russia) for 250 min. Acetylacetone (analytically pure grade, Merck, Darmstadt, Germany) (AcAc) was used as a dispersant. Concentration of the acetylacetone was chosen based on the calculation of the mass of acetylacetone per total surface area of nanoparticles in suspension according to the formula:

$$m_{AcAc} = \mu \cdot S_{sp} \cdot m_{np}, \quad (1)$$

where μ is the mass of acetylacetone per unit surface of the nanopowder, mg/m^2, the value was 1 mg/m^2 in these experiments; S_{sp} is the specific surface of the nanopowder (m^2/g); m_{np} is the mass of the nanopowder (g); m_{AcAc} is the mass of acetylacetone (mg).

The large particles in *80YLa* suspensions were removed by centrifugation with a Hermle Z383 centrifuge at a speed of 2000 rpm for 1 min. The concentration of the suspension after centrifugation was about 60 g/L. To reduce a probability of cracks formation at a stage of drying of the compacts, a polymer modifier, polyvinyl butyral (PVB), was introduced into the suspension as a binder in an amount of 1 mg/m^2.

Suspensions of *76YLa* at a concentration of 70 g/L was prepared in isopropanol and sonicated with an ultrasonic probe (Bandelin SONOPULS HD 3200, Germany) at frequency of 20 kHz and ultrasonic power of 40 W for 250 min. After the treatment AcAc (1 mg/m^2) was added. To prepare the *76YLa_milling* suspension, *76YLa* powder was used, which was subjected to two-stage grinding in a planetary mill (MPP-1, St. Petersburg) in isopropyl alcohol with ceramic zirconium balls of 5 mm in diameter at the first stage for 5 hours and 2 mm in diameter at the second stage for 5 hours, at a rotation speed of 320 rpm. The *76YLa_milling* suspension was prepared in the isopropanol with the addition of acetylacetone (1 mg/m^2), followed by ultrasonic treatment for 125 min (UZV-13/150-TN ultrasonic bath) and centrifugation at 2000 rpm for 1 min. The concentration of the deaggregated suspension was 58 g/L.

2.2. Nanopowders and Suspensions of $(Ho_{0.95}La_{0.05})_2O_3$

The $(Ho_{0.95}La_{0.05})_2O_3$ (*HoLa*) nanopowder was obtained by the method of self-propagating high-temperature synthesis (SHS). The process is described in detail in [8]. The materials to use for the SHS were holmium oxide (99.99% Polirit, Russia), lanthanum oxide (99.99% Polirit, Russia), nitric acid (99.9999%, Khimreaktiv, Russia) and glycine NH_2CH_2COOH (99.9%, Khimreaktiv, Russia). The powders received after SHS were annealed in air at a temperature of 900°C for 3 h. The *HoLa* powder was ground in a planetary mill (MPP-1, St. Petersburg) in isopropyl alcohol with ceramic zirconium balls of 5 mm in diameter at a rotation speed of 320 rpm for 5 h. Suspensions with an initial concentration of 70 g/L were sonicated using an ultrasonic bath (UZV-13/150-TN) for 125 min. Acetylacetone (1 mg/m^2) was used as a dispersant. Undestroyed large aggregates were removed by centrifugation of the suspensions with a Hermle Z383 centrifuge at a rotation speed of 1500 rpm for 1 min. The concentration of the deaggregated suspension was 62 g/L.

 doi:10.20944/preprints202308.2043.v1

2.3. Characterization of the Suspensions and Electrophoretic Deposition (EPD)

Electrokinetic measurements were performed by the electroacoustic method using a DT-300 analyzer (Dispersion Technology Inc, USA). All measurements for suspensions were carried out under isothermal conditions in air at 298 K.

2.3.1. Electrophoretic Deposition of One-Layer Compacts

Electrophoretic deposition was performed on a specialized computerized setup providing constant voltage regimes, which was developed and made at the Institute of Electrophysics, Ural Branch of Russian Academy of Sciences. The EPD was performed in a cell with a horizontal arrangement of electrodes. An aluminum foil disk with an area of 113 mm² was a cathode, and a stainless-steel disk served as an anode. A distance between the electrodes was 10 mm. To form bulk one-layer compacts by the EPD from nanoparticle suspensions, the following deposition modes were used: for suspensions of *76YLa* (3 samples) and *80YLa* (2 samples) powders the constant voltage was 20 V, for the *HoLa* suspensions (2 samples) – 40 V. The deposition time in all cases was 120–150 min. During the EPD, the suspensions were pumped from the bottom of the cell to its upper part. The green bodies deposited were dried on the cathode for 7 days in isopropyl alcohol vapor using a desiccator.

2.3.2. Electrophoretic Deposition of Two-Layers Compacts

To form two-layers compacts, the layer-by-layer EPD was performed from suspensions of either *76YLa* or *80YLa* powders at a constant voltage of 20 V for 120 min; then, the EPD was performed from the suspension of the *HoLa* powders at a constant voltage of 40 V for 90–150 min. Two samples of two-layer compacts were formed: 76YLa/HoLa and 80YLa/HoLa. During the EPD the suspension was pumped from the bottom of the cell to its upper part. The resulting green bodies were dried on the cathode for 7 days in isopropyl alcohol vapor using a desiccator.

2.4. Sintering of the Ceramics

Sintering of the ceramics was carried out in vacuum furnace SNVE 1.3.1–20 (OOO Prizma, Russia) with a tungsten heater at a pressure of about $1 \cdot 10^{-2}$ Pa, heating rate of 0.5°C/min, temperature of 1750°C and 10 h holding time at the maximum temperature. As our previous research demonstrated, the sintering conditions gave a chance to make ytterbium doped $(Y_{0.9}La_{0.1})_2O_3$ laser ceramics [25] and $(Ho_{0.95}La_{0.05})_2O_3$ magnetooptical ceramics [8] where the lanthana was used as a sintering aid. Disk samples were cut across the deposited layers and polished with a Phoenix Beta Grinder/Polisher (BUEHLER, Germany). Investigation of the samples was carried out with the help of a scanning electron microscope EVO LS 10 (Carl Zeiss, Germany). Sample surfaces were visualized using backscattered electron (BSE) and secondary electron (SE) imaging at accelerated voltages 5 and 20 kV. Elemental composition of samples was examined by an energy dispersive X-ray spectroscopy (EDS) with Inca Energy X-MAX^N 50 detector (Oxford Instruments, UK).

3. Results

3.1. Characteristics of $(Y_{0.9}La_{0.1})_2O_3$ Nanopowders and Suspensions

The harvested *YLa* powders contained weakly agglomerated spherical nanoparticles with a characteristic size of 15 – 20 nm. The morphology of nanoparticles and their size distribution are shown in [24]. In addition to the nanoparticles, the powder contained spherical particles with a characteristic size of 100 – 200 nm, formed as a result of spattering of a melted material in the focal spot of the laser radiation, and shapeless particles with a size of 10 – 100 μm, formed due to splitting of a crust from the target surface. The amount of such large particles in the powder collected in the electrostatic filter was about 1% wt., and in the powder collected in the cyclone – up to 10% wt. The micron-sized particles were removed during further processing by centrifugation of suspensions. A batch of *76YLa* powders was sieved with a 200 Mesh polymer sieve prior to further processing. The

Preprints (www.preprints.org) | NOT PEER-REVIEWED | Posted: 30 August 2023 doi:10.20944/preprints202308.2043.v1

specific surface area of the *YLa* nanopowders after annealing, determined by the BET method, was about 30 m^2/g. XRD analyses of the annealed nanopowders revealed the nanoparticles to be single-phase cubic structure of Y_2O_3 sesquioxides (space group *Ia-3*, a=10.68(2) Å).

The powder used to prepare the suspensions, the dispersant, the binder, and the value of the ζ-potential of the nanoparticles of the resulting suspensions are listed in Table 1.

Table 1. Composition of the suspensions and ζ-potential of the nanoparticles.

Powders	Dispersion medium	ζ–potential, mV
76YLa	iPrOH	+4
	iPrOH + AcAc (1 mg/m²)	+49
	iPrOH + AcAc (1 mg/m²) + PVB (1 mg/m²)	+29
76YLa_milling	iPrOH	+11
	iPrOH + AcAc (1 mg/m²)	+49
80YLa	iPrOH	+13
	iPrOH + AcAc (1 mg/m²)	+69
	iPrOH + AcAc (1 mg/m²) + PVB (1 mg/m²)	+67
HoLa	iPrOH	+16
	iPrOH + AcAc (1 mg/m²)	+86
	iPrOH + AcAc (1 mg/m²) + PVB (1 mg/m²)	+80

The suspension was treated with the ultrasonic probe for 5 min (*76YLa_AcAc*). The concentration of the *76YLa_AcAc* suspension after centrifugation (2000 rpm, 1 min) was 64 g/L. The *76YLa_PVB* suspension was prepared by introducing PVB (1 mg/m²) into the *76YLa_AcAc* suspension after electrophoretic precipitation of the *76YLa_1* sample (Table 2).

Additionally, aging of the *76YLa_PVB* and *80YLa* suspensions for 14 days was studied, which is of interest from the point of view of the practical application of EPD technology, which should withstand the use of stable suspensions for a long time. During the study of the aging, the suspension was stored in a dark place at room temperature for 14 days.

Table 2. Suspensions and parameters of the EPD of one-layer compacts.

Sample	**Suspension**	**Dispersion medium**	**Mode of the EPD (voltage, time); Mass / thickness / density of the green body**
76YLa_1	76YLa_AcAc	iPrOH/AcAc	20 V, 150 min; 440 mg / 1.6 mm / 43%
76YLa_2	76YLa_PVB aged for 14 days	iPrOH/AcAc/PVB	20 V, 150 min; 175 mg / 1 mm / 32%
76YLa_3	76YLa_milling	iPrOH/AcAc	20 V, 150 min; 524 mg / 2.5 mm / 37%
80YLa_1	80YLa	iPrOH/AcAc/PVB	20 V, 120 min; 250 mg / 1.5 mm / 38%
80YLa_2	80YLa aged for 14 days	iPrOH/AcAc/PVB	20 V, 120 min; 171 mg / 1.0 mm / 32%
HoLa_1	HoLa_AcAc	iPrOH/AcAc	40 V, 120 min; 751 mg/ 1,9 mm / 30%
HoLa_2	HoLa_PVB	iPrOH/AcAc/PVB	40 V, 120 min; 447 mg / 1.5 mm / 32%

3.2. Characteristics of $(Ho_{0.95}La_{0.05})_2O_3$ Nanopowders and Suspensions

The specific surface area of the *HoLa* nanopowder after annealing, determined by the BET method, was 18 m^2/g. The powder consists of a mixture of large particles with sizes of hundreds of nanometers, and small nanometers size particles. Morphology of nanoparticles of $(Ho_{1-x}La_x)_2O_3$ solid

solutions made by the SHS and their size distribution are given in [8]. XRD analysis of the nanopowders shows a C-type cubic structure of Ho_2O_3 sesquioxides (space group *Ia-3*, No. 206, Z = 16). No second phases were found in the powders. Composition of the suspensions prepared and ζ-potential of the *HoLa* nanoparticles are given in Table 1. The used suspensions, the EPD parameters and characteristics of the obtained one-layers and two-layers compacts are shown in Table 2 and Table 3, respectively.

Table 3. Suspensions and parameters of the EPD of two-layers compacts.

Sample	Suspension	Dispersion medium	Mode of the EPD (voltage, time); Mass / thickness / fraction of the layer	Density of the green body, % of theoretical*
76YLa/HoLa_1	76YLa_milling	iPrOH/AcAc	20 V, 120 min; 570 mg / 1.6 mm / 0.62	46
	HoLa_PVB	iPrOH/AcAc/PVB	40 V, 150 min; 356 mg / 1.0 mm / 0.38	
80YLa/HoLa_2	80YLa_PVB	iPrOH/AcAc/PVB	20 V, 120 min; 266 mg / 0.7 mm / 0.58	46
	HoLa_PVB	iPrOH/AcAc/PVB	40 V, 90 min; 190 mg / 0.5 mm / 0.42	

***Note:** The layer fraction for the two-layers compact is defined as the ratio of the thickness of the deposited layer to the total thickness of the two-layers compact.

4. Discussion

To obtain the bulk compacts by electrophoretic deposition, a high aggregation stability of the suspensions is required. In the case of electrostatic stabilization, the stability is directly related to the ζ-potential of nanoparticles. From Table 1 it is seen that the initial suspensions in isopropanol are characterized by low values of the ζ-potential (+4…+16 mV). Previous experiments on the EPD of nanoparticles from isopropanol suspensions [24] showed the necessity to use a dispersant, because without it, when the electric field was applied, the flocculation process began in the suspension and rather quickly the entire nanopowder settled to the bottom of the cuvette. When acetylacetone, used in this study as a dispersant, is added, the zeta potential of nanoparticles increases significantly (+49...+86 mV), which is due to an increase in the surface charge of the particles because of adsorption of protons formed during the dissociation of the enol form of acetylacetone on surface of the nanoparticles [29]. When PVB, used as a binder, is added to the suspension, the zeta potential of the nanoparticles decreases (Table 1). The authors of [26] reported a similar effect of reducing the zeta potential when PVB was added to a suspension based on zirconium dioxide. The decrease in the ζ-potential may be due to the adsorption of PVB molecules on the particle surface, which prevents the adsorption of protons. At the same time, despite the effect of PVB on the electrokinetic parameters, the values of the ζ-potential still exceeded in absolute value the characteristic value of 26 mV, which is necessary for the stable conduction of the EPD process [27].

4.1. Electrophoretic Deposition of Single-Layer Compacts from Suspensions of the YLa Nanopowders

Figure 1 shows dependences of the current strength on the time of the EPD from suspensions of *76YLa* powder in isopropanol with acetylacetone (1 mg/m²) without a binder (*76YLa_AcAc*) and with the addition of PVB (*76YLa_PVB*). It can be seen that the dependences of the current strength on the EPD time do not have a clearly pronounced downward trend associated with the depletion of the suspensions during the EPD process, which indicates a predominantly ionic nature of the charge transfer. Moreover, in the *76YLa_AcAc* suspension for about 60 min. there is an increase in the current (about 10%), which is associated with an increase in the concentration of ions in the medium, apparently due to processes occurring on the electrodes. Only after 110 minutes of the EPD, the

Preprints (www.preprints.org) | NOT PEER-REVIEWED | Posted: 30 August 2023 doi:10.20944/preprints202308.2043.v1

processes of increasing the electrical resistance of the layer of nanoparticles deposited on the cathode and reducing the concentration of the nanoparticles remained in the suspension begin to affect the current value. The significant effect of the PVB addition on the conductivity of the suspension (curve 2, Figure 1) is obviously associated both with a decrease in the ζ-potential of nanoparticles (the values of the ζ-potential and electrophoretic mobility are directly proportional, according to the Henry equation [28]) and with higher resistivity of the layer deposited. It can be seen that in the first minutes (sometime tens of seconds) of the formation of a layer of the nanoparticles on the cathode, there is a rapid drop in the value of the current, and then, for about 40 min. additional reduction of the current by another 20%.

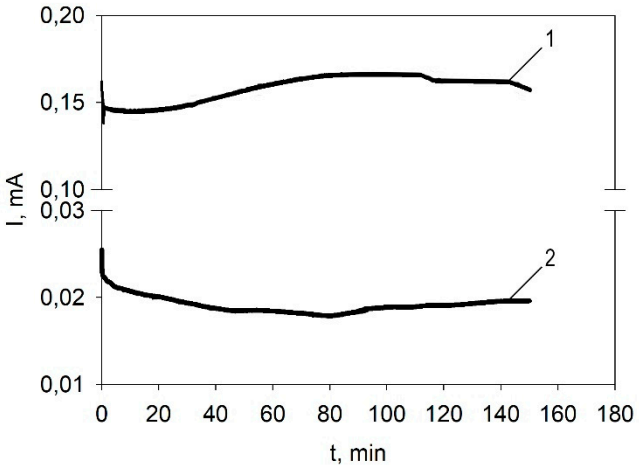

Figure 1. Dependence of the current on the EPD time (electric field strength of 20 V/cm) in suspensions: *76YLa_AcAc* without a binder (sample *76YLa_1*, curve 1) and *76YLa_PVB* with PVB addition (sample *76YLa_2*, curve 2).

Figure 2 shows the dependences of the current strength on the time of the EPD from suspensions of *80YLa_PVB* in isopropanol with acetylacetone (1 mg/m^2) with the addition of PVB binder (1 mg/m^2) freshly prepared and aged for 14 days. It can be seen that the dependences have a similar character, for which the current value is approximately constant for 120 min. It should be noted that when the suspension was aged for 14 days, there was a significant (4 times) increase in the current (Figure 2, curve 2), which may be due to a change in the ionic composition of the dispersion medium because of formation of complex compounds, namely, metal acetylacetonates with the release of protons, which has a significant effect on the conductivity of the suspension [29]. However, when EPD from *80YLa_PVB* suspension was made, aging of the suspension had a negative effect: there was a decrease in the mass, thickness and density of the *80YLa_2* sample (Table 2), despite the higher current during the EPD (Figure 2).

Preprints (www.preprints.org) | NOT PEER-REVIEWED | Posted: 30 August 2023 doi:10.20944/preprints202308.2043.v1

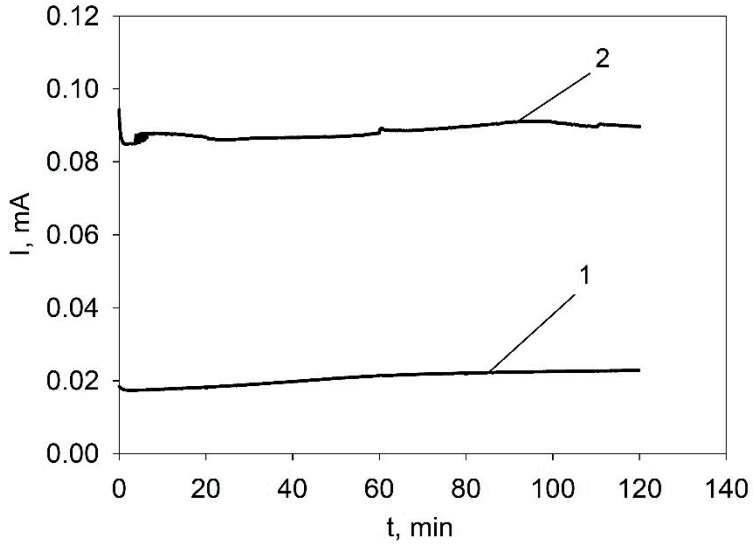

Figure 2. Dependences of the current on the time of the EPD (electric field strength of 20 V/cm) from *80YLa_PVB* suspension: freshly prepared (sample *80YLa_1*, curve 1) and aged for 14 days (sample *80YLa_2*, curve 2).

Single layer compacts *76YLa_1*, *76YLa_2*, and *76YLa_3* were obtained under the same EPD conditions from suspensions of *76YLa_AcAc*, *76YLa_PVB*, and *76YLa_milling*, respectively. From Table 2 it's seen that samples with the largest mass and thickness were obtained from suspensions without the addition of the PVB. The addition of a polymeric binder led to a decrease in the thickness and weight of the samples, however, upon drying, the *76YLa_2* sample deposited from a suspension with the addition of the PVB retained its integrity, in contrast to the samples without the PVB. Sample *76YLa_3*, deposited from a suspension of *76YLa_milling* powder, had the highest tendency to crack upon drying.

4.2. Electrophoretic Deposition of One-Layer Compacts from Suspensions of HoLa Nanopowder

Preliminary experiments on the EPD from a suspension of *HoLa* powder revealed that at electric field strength of 20 V/cm there was no deposition (mass growth on the electrode) from the *HoLa* suspension, therefore, subsequent experiments were carried out at a field strength of 40 V/cm. Figure 3 shows dependences of the current on the time of the EPD from suspensions of *HoLa* nanopowder in the dispersion medium of isopropanol with acetylacetone (1 mg/m^2) without the addition of a binder (*HoLa_AcAc*) and with the addition of PVB (*HoLa_PVB*). From Figure 3 it can be seen that the magnitude of the current during the EPD changes insignificantly. The EPD current values for the *HoLa_AcAc* suspension (I_{av} = 0.338 mA) are higher than for the *HoLa_PVB* suspension (I_{av} = 0.184 mA).

Electrophoretic deposition of samples of one-layer compacts *HoLa_1* and *HoLa _2* was carried out in the same modes from suspensions of *HoLa_AcAc* and *HoLa_PVB*, respectively. From Table 2 it can be seen that the introduction of PVB into the suspension of *HoLa* nanopowder led, as in the case of suspensions of yttrium oxide nanopowders, to a decrease in the mass and thickness of the compact (sample *HoLa_2*).

Preprints (www.preprints.org) | NOT PEER-REVIEWED | Posted: 30 August 2023 doi:10.20944/preprints202308.2043.v1

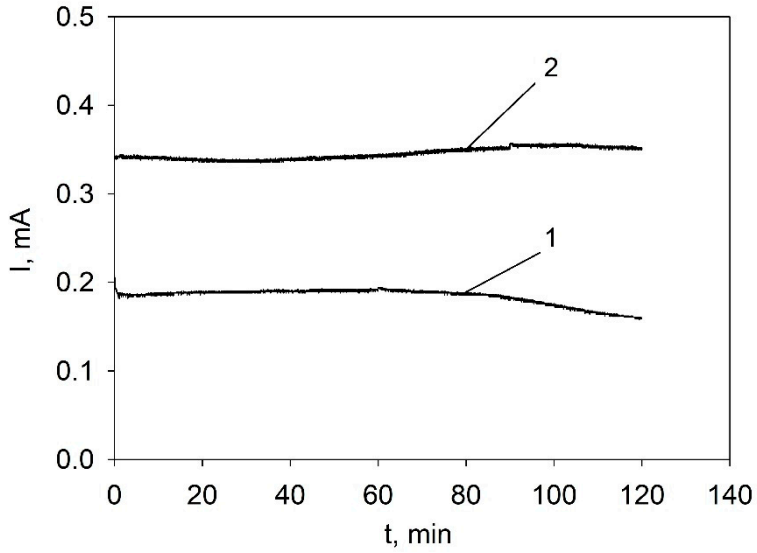

Figure 3. Dependences of the current on time during the EPD (electric field strength of 40 V/cm) from *HoLa_PVB* suspension with the addition of PVB (sample *HoLa_2*, curve 1) and *HoLa_AcAc* without the addition of a binder (sample *HoLa_1*, curve 2).

4.3. Electrophoretic Deposition of Two-Layers Compacts

Figure 4 shows the kinetics of the current during the electrophoretic deposition of the two-layers compacts *76YLa/HoLa_1* and *80YLa/HoLa_2*. It can be seen that during the EPD of the first *76YLa* layer of the *76YLa/HoLa_1* sample, the current slightly increases with increasing time from 0.145 to 0.162 mA (Figure 4a). During the EPD of the second *HoLa* layer, there is a fairly obvious tendency for the current to decrease by a factor of 1.8 from 0.294 to 0.166 mA, which is associated with an increase in the electrical resistance of the layer deposited on the cathode.

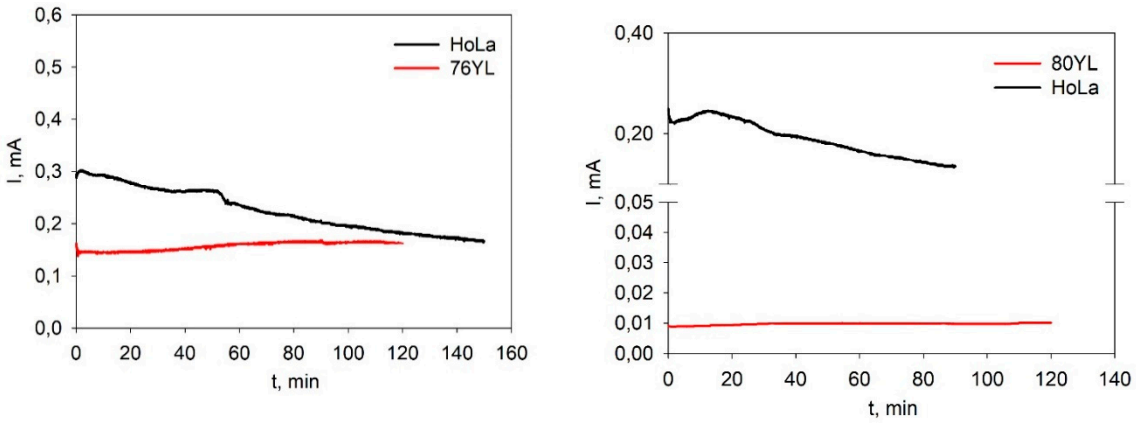

(a) **(b)**

Figure 4. Dependences of the current on time during the EPD of two-layers samples: **(a)** *76YLa/HoLa_1* and **(b)** *80YLa/HoLa_2*.

In the case of deposition of the two-layers compact from suspensions with PVB during the EPD of the first *80YLa* layer of the *80YLa/HoLa_2* sample, the current remains almost constant (Figure 4b). At the stage of the EPD of the second *HoLa* layer, the current decreases by a factor of 2 from 0.250 to 0.135 mA.

Preprints (www.preprints.org) | NOT PEER-REVIEWED | Posted: 30 August 2023 doi:10.20944/preprints202308.2043.v1

The mass of the *80YLa/HoLa_2* sample was 456 mg and thickness of 1.2 mm with a density of 46%, while *76YLa/HoLa_1* sample with the same density of 46% was characterized by the largest mass, equal to 926 mg and a thickness of 2.6 mm. Obviously, the increase in the mass and thickness of the *76YLa/HoLa_1* sample is due to the use of a suspension based on the *76YLa* powder without the addition of PVB during the deposition of the first layer (Table 3). As noted earlier in the case of the deposition of the one-layer compacts, the introduction of the PVB into the suspensions of nanoparticles leads to a decrease in the mass and thickness of the samples.

Figure 5 shows a sample of the two-layers compact after deposition and drying. It can be seen that the sample is characterized by good uniformity of the deposited layers.

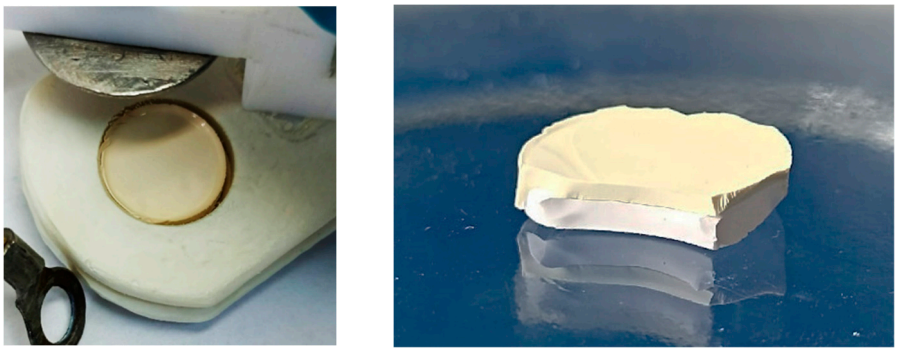

(a) **(b)**

Figure 5. Two-layers compact formed by the EPD: **(a)** in the EPD cell, **(b)** after drying.

The obtained two-layers compacts were sintered in vacuum at a temperature of 1750°C for 10 h. The heating rate was 0.5°C/min. The characteristic size of crystallites in the obtained ceramics was 15 – 20 μm. In samples where the *YLa* layer did not contain PVB (*76YLa/HoLa_1*), cracks appeared in the longitudinal plane after sintering. Samples that contain the PVB in both layers remained uniform after the vacuum sintering. Figure 6a (high-resolution picture is attached as a Supplementary File to this paper) shows a micrograph of a cross section of the *80YLa/HoLa_2* sample. The distribution of chemical elements over the depth of the sample is shown in Figure 6b. Since the images were obtained by collecting backscattered electrons, the darker region corresponds to materials with lower density, in this case – $(Y_{0.9}La_{0.1})_2O_3$, which has density of 5.2 g/cm^3 (in comparison with $(Ho_{0.95}La_{0.05})_2O_3$ – 8.3 g/cm^3). Thickness of the layer with interdiffused ions is about 30 μm.

The resulting ceramics demonstrate complete sintering of the *YLa/HoLa* layers, low porosity of the *HoLa* layer, and a relatively high content of pores with characteristic sizes of a few microns at crystallite boundaries in the *YLa* layer (Figure 6a). It is known that such pores in optical ceramics can be eliminated by either significantly increasing the sintering time or using additional hot isostatic pressing (HIP) [15,30]. Two facts are worth additional discussion:

1. Close to the *YLa/HoLa* interface, after the sintering, micron-sized pores were formed, located almost in the same plane. It is possible that the appearance of these pores is associated with air bubbles that appeared on the surface of the deposited *YLa* layer at the moment of transfer of the sample to the *HoLa* suspension and remained in the two-layers compact after drying. In this case, their appearance can be avoided by adjusting the process of the sample movement between the suspensions.

2. If the assumption that the pores are located at the boundary of the deposited layers is correct, then it follows from the ion distributions (Figure 6b) that during the sintering, predominant (almost one-sided) diffusion of holmium ions into the Y_2O_3 lattice occurs. Taking into account the proximity of the ionic radii of Ho^{3+} and Y^{3+} in the cubic lattice of the sesquioxides (1.015 Å and 1.019 Å, respectively), as well as the presence of La^{3+} ions and the fact that, during the sintering, diffusion proceeds primarily along crystallite boundaries, weak diffusion of yttrium ions into the *HoLa* layer is difficult to explain. It is possible that such a shift in the distribution of chemical elements is associated not with the diffusion processes during the sintering, but with the incorporation of *HoLa*

Preprints (www.preprints.org) | NOT PEER-REVIEWED | Posted: 30 August 2023 doi:10.20944/preprints202308.2043.v1

nanoparticles into the *YLa* layer at the initial stage of the EPD of the second layer. Indeed, the *HoLa* nanoparticles accelerated by an electric field in suspension can be driven deep into the *YLa* layer deposited at the first stage of the EPD.

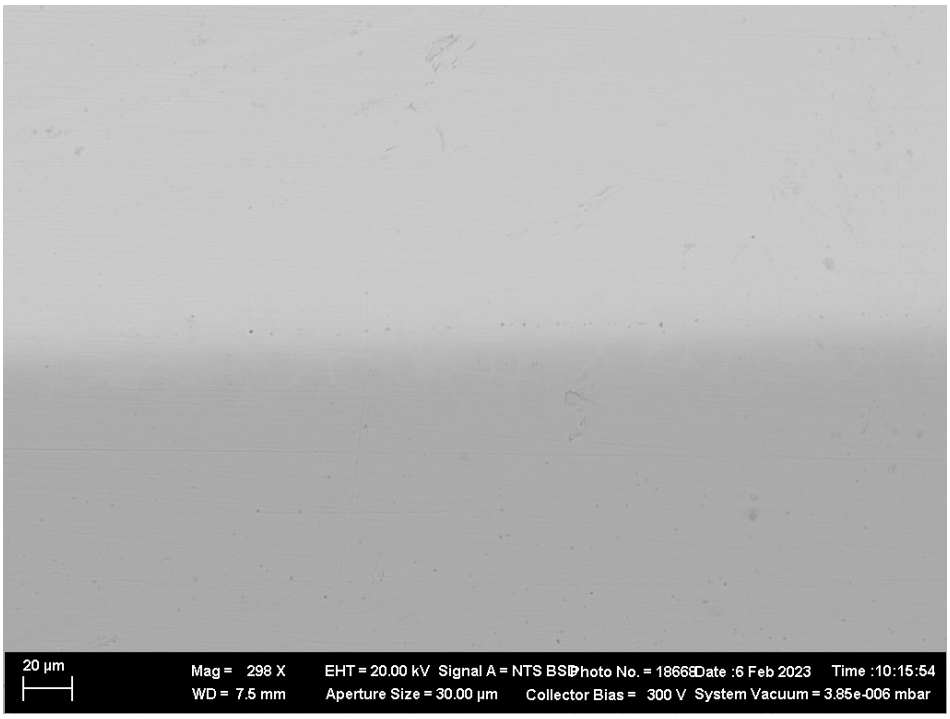

(a)

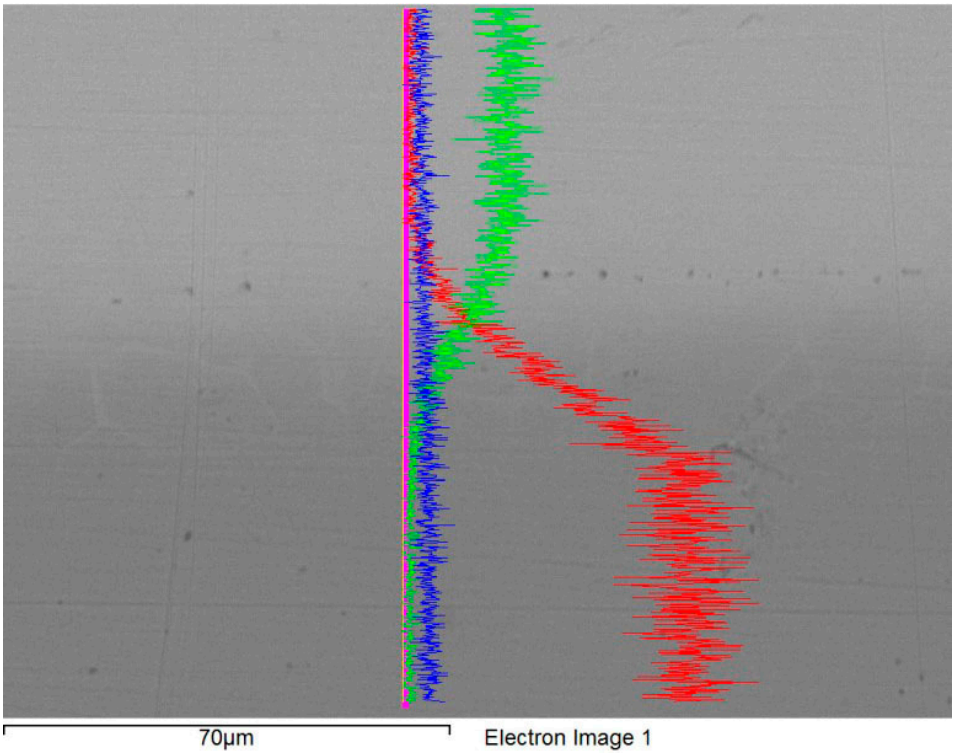

(b)

Figure 6. Micrograph of cross section of the *80YLa/HoLa_2* sample **(a)** and the distribution of chemical elements **(b)**: yttrium (red), holmium (green) and lanthanum (blue).

5. Conclusions

The use of acetylacetone and PVB made it possible to obtain stable suspensions of $(Y_{0.9}La_{0.1})_2O_3$ and $(Ho_{0.95}La_{0.05})_2O_3$ nanopowders, characterized by high ζ–potential (+29…+80 mV), which gives a chance to carry out a stable EPD process and make a bulk ceramic green body. One-layer compacts of the *YLa* and *HoLa* nanopowders with a density of 30–43% were formed from the nanopowder suspensions by the electrophoretic deposition. It was found out that the introduction of the PVB into the suspensions leads to a decrease in the mass and thickness of the compacts, but does not significantly affect their density. Two-layers *YLa*/*HoLa* compacts were made by the layer-by-layer electrophoretic deposition. It is shown that with the help of the EPD method it is possible to form the two-layers compacts with a thickness of up to 2.6 mm and a density of up to 46 %. Sintering such compacts in a vacuum at a temperature of 1750°C leads to the formation of ceramics with a homogeneous boundary between the *YLa*/*HoLa* layers, which have a thickness of the layer with interdiffused ions of about 30 μm. The ceramics show residual porosity in the *YLa* layer and at the interface between the deposited *YLa*/*HoLa* layers. It can be expected that these pores with a characteristic size of a few microns will be eliminated with an increase in the sintering time or additional HIP treatment of ceramics.

Acknowledgments: The research performed by Ivanov M.G. and Kalinina E.G. in a part of the EPD of the samples was funded by the Russian Science Foundation (research project No. 18-13-00355). A part of the research performed by Kundikova N.D. was funded by the Ministry of Science and Higher Education (No. 122011200363-9). The scanning electron microscopy, performed in the Ural Center for Shared Use "Modern nanotechnology" Ural Federal University (Reg.№ 2968) was funded by the Ministry of Science and Higher Education (Project № 075-15-2021-677).

References

1. I. Snetkov, J. Li, Selection of Magneto-Optical Material for a Faraday Isolator Operating in High-Power Laser Radiation, Magnetochemistry. 8 (2022) 168. https://doi.org/10.3390/magnetochemistry8120168.
2. A. Ikesue, Y.L. Aung, Synthesis and Performance of Advanced Ceramic Lasers, Journal of the American Ceramic Society. 89 (2006) 1936–1944. https://doi.org/10.1111/j.1551-2916.2006.01043.x.
3. F. Tang, Y. Cao, J. Huang, H. Liu, W. Guo, W. Wang, Fabrication and Laser Behavior of Composite Yb:YAG Ceramic, Journal of the American Ceramic Society. 95 (2012) 56–69. https://doi.org/10.1111/j.1551-2916.2011.04956.x.
4. K. Fujioka, X. Guo, M. Maruyama, J. Kawanaka, N. Miyanaga, Room-temperature bonding with post-heat treatment for composite Yb:YAG ceramic lasers, Opt Mater (Amst). 91 (2019) 344–348. https://doi.org/10.1016/j.optmat.2019.03.032.
5. I. Mukhin, E. Perevezentsev, O. Palashov, Fabrication of composite laser elements by a new thermal diffusion bonding method, Opt Mater Express. 4 (2014) 266. https://doi.org/10.1364/OME.4.000266.
6. E.R. Kupp, G.L. Messing, J.M. Anderson, V. Gopalan, J.Q. Dumm, C. Kraisinger, N. Ter-Gabrielyan, L.D. Merkle, M. Dubinskii, V.K. Simonaitis-Castillo, G.J. Quarles, Co-casting and optical characteristics of transparent segmented composite Er:YAG laser ceramics, J Mater Res. 25 (2010) 476–483. https://doi.org/10.1557/JMR.2010.0069.
7. H. Ichikawa, K. Yamaguchi, T. Katsumata, I. Shoji, High-power and highly efficient composite laser with an anti-reflection coated layer between a laser crystal and a diamond heat spreader fabricated by room-temperature bonding, Opt Express. 25 (2017) 22797. https://doi.org/10.1364/OE.25.022797.
8. S. Balabanov, S. Filofeev, M. Ivanov, A. Kaigorodov, D. Kuznetsov, D.J. Hu, J. Li, O. Palashov, D. Permin, E. Rostokina, I. Snetkov, Fabrication and characterizations of holmium oxide based magneto-optical ceramics, Opt Mater (Amst). 101 (2020) 109741. https://doi.org/10.1016/j.optmat.2020.109741.
9. L. Jin, G. Zhou, S. Shimai, J. Zhang, S. Wang, ZrO2-doped Y2O3 transparent ceramics via slip casting and vacuum sintering, J Eur Ceram Soc. 30 (2010) 2139–2143. https://doi.org/10.1016/j.jeurceramsoc.2010.04.004.
10. S.K. Dutta, G.E. Gazza, Transparent Y2O3 by hot-pressing, Mater Res Bull. 4 (1969) 791–796. https://doi.org/10.1016/0025-5408(69)90001-4.

11. K. Majima, N. Niimi, M. Watanabe, S. Katsuyama, H. Nagai, Effect of LiF addition on the preparation of transparent Y2O3 by the vacuum hot pressing method, J Alloys Compd. 193 (1993) 280–282. https://doi.org/10.1016/0925-8388(93)90371-S.
12. S. Balabanov, S. Filofeev, A. Kaygorodov, V. Khrustov, D. Kuznetsov, A. Novikova, D. Permin, P. Popov, M. Ivanov, Hot pressing of Ho2O3 and Dy2O3 based magneto-optical ceramics, Optical Materials: X. 13 (2022) 100125. https://doi.org/10.1016/j.omx.2021.100125.
13. A. Ikesue, K. Kamata, K. Yoshida, Synthesis of Transparent Nd-doped HfO2-Y2O3 Ceramics Using HIP, Journal of the American Ceramic Society. 79 (1996) 359–364. https://doi.org/10.1111/j.1151-2916.1996.tb08129.x.
14. J. Mouzon, A. Maitre, L. Frisk, N. Lehto, M. Odén, Fabrication of transparent yttria by HIP and the glass-encapsulation method, J Eur Ceram Soc. 29 (2009) 311–316. https://doi.org/10.1016/j.jeurceramsoc.2008.03.022.
15. D. Hu, X. Li, L. Zhang, I. Snetkov, P. Chen, Z. Dai, S. Balabanov, O. Palashov, J. Li, Terbium (III) Oxide (Tb2O3) Transparent Ceramics by Two-Step Sintering from Precipitated Powder, Magnetochemistry. 8 (2022) 73. https://doi.org/10.3390/magnetochemistry8070073.
16. Y. Xin, T. Xu, Y. Wang, P. Luo, W. Li, B. Kang, B. Mei, W. Jing, Effect of ZrO2 Content on Microstructure Evolution and Sintering Properties of (Tb0.7Lu0.3)2O3 Magneto-Optic Transparent Ceramics, Magnetochemistry. 8 (2022) 175. https://doi.org/10.3390/magnetochemistry8120175.
17. D. Yin, J. Wang, M. Ni, P. Liu, Z. Dong, D. Tang, Fabrication of Highly Transparent Y2O3 Ceramics with CaO as Sintering Aid, Materials. 14 (2021) 444. https://doi.org/10.3390/ma14020444.
18. R. Chaim, A. Shlayer, C. Estournes, Densification of nanocrystalline Y2O3 ceramic powder by spark plasma sintering, J Eur Ceram Soc. 29 (2009) 91–98. https://doi.org/10.1016/j.jeurceramsoc.2008.05.043.
19. N. Frage, S. Cohen, S. Meir, S. Kalabukhov, M.P. Dariel, Spark plasma sintering (SPS) of transparent magnesium-aluminate spinel, J Mater Sci. 42 (2007) 3273–3275. https://doi.org/10.1007/s10853-007-1672-0.
20. K.A. Appiagyei, G.L. Messing, J.Q. Dumm, Aqueous slip casting of transparent yttrium aluminum garnet (YAG) ceramics, Ceram Int. 34 (2008) 1309–1313. https://doi.org/10.1016/j.ceramint.2007.03.010.
21. M. Bredol, J. Micior, S. Klemme, Electrophoretic deposition of alumina, yttria, yttrium aluminium garnet and lutetium aluminium garnet, J Mater Sci. 49 (2014) 6975–6985. https://doi.org/10.1007/s10853-014-8403-0.
22. B.V. Derjaguin, S.S. Dukhin, V.N. Shilov, Kinetic aspects of electrochemistry of disperse systems. Part I. Introduction, Adv Colloid Interface Sci. 13 (1980) 141–152. https://doi.org/10.1016/0001-8686(80)87004-7.
23. M. Ivanov, E. Kalinina, Y. Kopylov, V. Kravchenko, I. Krutikova, U. Kynast, J. Li, M. Leznina, A. Medvedev, Highly transparent Yb-doped (La<inf>x</inf>Y<inf>1 − x</inf>)<inf>2</inf>O<inf>3</inf>ceramics prepared through colloidal methods of nanoparticles compaction, J Eur Ceram Soc. 36 (2016). https://doi.org/10.1016/j.jeurceramsoc.2016.06.013.
24. E. Kalinina, M. Ivanov, The Electrophoretic Deposition of Nanopowders Based on Yttrium Oxide for Bulk Ceramics Fabrication, Inorganics (Basel). 10 (2022) 243. https://doi.org/10.3390/inorganics10120243.
25. M. Ivanov, Y. Kopylov, V. Kravchenko, S. Zayats, Sintering and optical quality of highly transparent yb-doped yttrium lanthanum oxide ceramics, Physica Status Solidi (C) Current Topics in Solid State Physics. 10 (2013). https://doi.org/10.1002/pssc.201300012.
26. M. Della Negra, S.P.V. Foghmoes, T. Klemensø, Complementary analysis techniques applied on optimizing suspensions of yttria stabilized zirconia, Ceram Int. 42 (2016) 14443–14451. https://doi.org/10.1016/j.ceramint.2016.06.046.
27. S. Bhattacharjee, DLS and zeta potential – What they are and what they are not?, Journal of Controlled Release. 235 (2016) 337–351. https://doi.org/10.1016/j.jconrel.2016.06.017.
28. D. Henry, The cataphoresis of suspended particles. Part I.—The equation of cataphoresis, Proceedings of the Royal Society of London. Series A, Containing Papers of a Mathematical and Physical Character. 133 (1931) 106–129. https://doi.org/10.1098/rspa.1931.0133.
29. Y. Nakamura, K. Isobe, H. Morita, S. Yamazaki, S. Kawaguchi, Metal complexes containing acetylacetone as a neutral ligand, Inorg Chem. 11 (1972) 1573–1578. https://doi.org/10.1021/ic50113a024.
30. X. Zhang, X. Huang, Z. Liu, Y. Feng, N. Jiang, L. Wu, Z. Yang, T. Xie, J. Li, Fabrication, microstructure and properties of transparent Yb:Y2O3 ceramics from co-precipitated nanopowders, Opt Mater (Amst). 122 (2021) 111792. https://doi.org/10.1016/j.optmat.2021.111792.

 doi:10.20944/preprints202308.2043.v1